Paleostress transition by fault-striation analysis in the northern and central Ryukyu arc, southwest Japan

Bull. Fac. Sci., Univ. Ryukyus, No. 78 : 163 – 231 (2004)

Paleostress transition by fault-striation analysis in the northern and central Ryukyu arc, southwest Japan

Noriaki TERAMAE and Daigoro HAYASHI

Department of Physics and Earth Sciences, University of the Ryukyus,
Nishihara, Okinawa, 903-0123, Japan

Abstract

The Ryukyu arc is an active arc-trench system, associate with active intracontinental back-arc basin (Okinawa Trough). Rifting of the Okinawa Trough has occurred since Miocene. The Ryukyu arc is expected to undergo complex geological history. Paleostress fields of the central and northern Ryukyu island are estimated from fault analysis by use of the Multi-inverse method (Yamaji, 2000) and Ginkgo method (Yamaji, 2003a).

The stress transition since middle Miocene is found by measurement of the fault-slip data in the northern and central Ryukyu arc. The fault-striation analysis leads the following tectonic evolution in the central and northern Ryukyu arc.

In middle Miocene, E-W extension occurred in the northern Ryukyu arc, which may be related to the opening of the Japan Sea. The compressional stress field occurred in late Miocene to early Pliocene (5-8 Ma), which was simultaneous with the formation of the Taiwan-Shinji Fold Belt. Subsequently E-W extension occurred in Pliocene, which was related to the opening the Okinawa Trough. Around at 2 Ma, complex stress regime occurred in the Ryukyu arc. In this time, opening of the Okinawa Trough resumed and the deposition of the Ryukyu group started. In northern Ryukyu arc, strike-slip stress regime has occurred from 2 Ma ago. NE-SW extension, arc-parallel extension is the latest stress regime in the central and northern Ryukyu arc. Arc parallel extension is observed in the whole Ryukyu arc. On the other hand, before the deposition of the Ryukyu group, stress regime of the southern Ryukyu arc is different from the central and northern Ryukyu arc.

1. Introduction

The Ryukyu arc is an active arc-trench system, which is characterized by the subduction of the Philippine Sea plate beneath the Eurasia plate (Fig.1). This area is an interesting field because Ryukyu arc has an active intracontinental back-arc basin, called the Okinawa Trough (Uyeda, 1977). The Okinawa Trough, which is expanding in present,

Received: June 29, 2004

runs parallel to the western Ryukyu arc in the East China Sea, and is considered the back-arc basin of the Ryukyu arc (Kimura, 1985; Letouzey and Kimura, 1985, 1986; Sibuet et al., 1987). Rifting of the Okinawa Trough has occurred since the Miocene (Letouzey and Kimura, 1986; Sibuet et al., 1987). The Okinawa Trough is considered to play an important role in stress history of the Ryukyu arc.

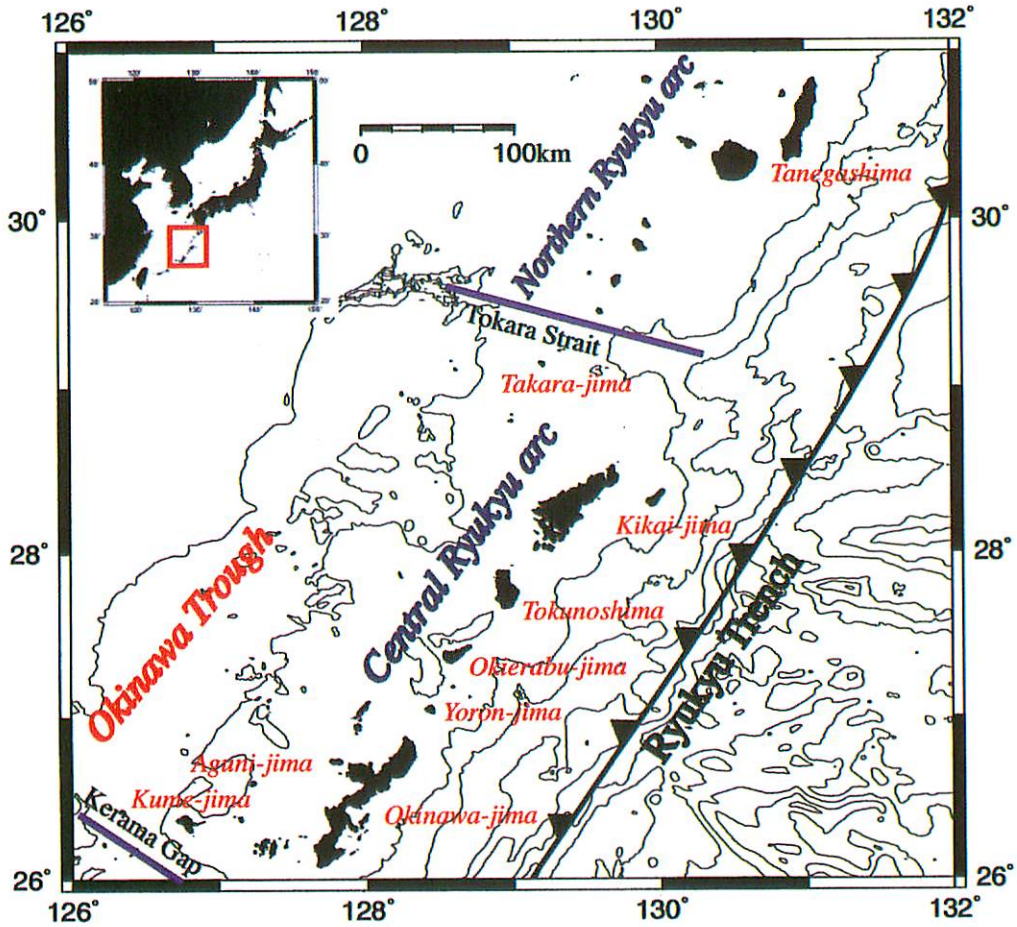

Fig.1. Tectonic setting of the northern and central Ryukyu area.

The Ryukyu arc is expected to undergo complex geological history. For instance, in Okinawa-jima, the tectonic event called "Uruma movement" is assumed because Quaternary sediments cut by steep faults (Kizaki, 1986).

In order to discuss the tectonics of the Ryukyu arc, it is important to estimate the paleostress state. The research about the transition of paleostress in this area is still uncertain. Fault striation analysis is a technique to estimate the paleostresses from the orientations and slip direction of meso-scale faults (Yamaji, 2001). The paleostress field in the Ryukyu arc has been studied by fault analysis using various methods (Kuramoto and

Konishi, 1989; Fabbri and Founier, 1999; Fabbri, 2000; Fournier et al., 2001; Otsubo and Hayashi, 2001; Teramae and Hayashi, 2002; Otsubo and Hayashi, 2003).

In the southern Ryukyu arc, Kuramoto and Konishi (1989) carried out fault analysis using the conjugate fault method, and they proposed new tectonics, which is attributed to the westward migration of the microplate. The initiation of this migration is proposed at 4 Ma, when the Philippine Sea plate motion changed its direction from N-S to NW-SE. However, the method of this study has several problems. The stress direction of obtained by this method is correct only in a special case, because this method assume that all faults occurred in the same tectonic event, and are conjugate fault. But many faults are not always conjugated.

Fabbri and Founier (1999) have studied in the southern Ryukyu arc using the classic inversion method. In Tanegashima, Fabbri (2000) has detected plaeostress field by the same method. In addition, Fournier et al. (2001) have studied in the southern area of the Okinawa-jima. The popular and classic inversion method (Angelier, 1979; 1984; 1990) has assumption, which all faults occurred by one stress state. It is a difficult task to separate stresses from the heterogeneous fault-slip data (Yamaji, 2001). However, the Ryukyu arc has undergone a complex stress field.

Otsubo and Hayashi (2001) studied on the basis of the classic inversion method in Miyako-jima. In this study, fault-striation of the Ryukyu group was observed. Previous researchers have not obtained fault-slip data from the Ryukyu Group in Ryukyu arc (Kuramoto and Konishi, 1989; Fabbri and Founier, 1999; Fournier et al., 2001).

Teramae and Hayashi (2002) studied on the basis of the classic inversion method in the Shimajiri group of southern area of the Okinawa-jima. This study tried the separation of the fault-slip data by the angular misfits between observed and predicted slip directions, which detected four stress states.

Recently, effective numerical methods have been proposed to separate stresses from polyphase fault-slip data (Yamaji, 2000; Yamaji, 2003a; etc.). According to the new method (Multi-inverse method and Ginkgo method), Otsubo and Hayashi (2003) have studied paleostresses in southern Ryukyu arc while in the northern and central Ryukyu arc have not yet done.

The purpose of this study is to reconstruct the detailed paleostresss field by the fault-striation analysis using Multi-inverse method and Ginkgo method, and to provide information on the deformation history of the Ryukyu arc caused by the rifting of the Okinawa Trough.

2. Geological setting

The Ryukyu arc is located between Kyushu and Taiwan for a distance of 1200 km along the margin of the western Pacific Ocean (Fig. 1). From the Pacific side to the continental margin, the Ryukyu trench, Ryukyu arc, volcanic front and the Okinawa

Trough are situated with their strikes parallel (Kizaki, 1986). The Ryukyu trench is the plate boundary between the Eurasia plate to the west and the Philippine Sea plate to the east. The Okinawa Trough has been the site of crustal stretching and thinning since the Miocene (Aiba and Sekiya, 1979; Letouzey and Kimura, 1985).

The Ryukyu arc is divided into three groups, which are bounded by Tokara Channel and Kerama Gap, respectively (Konishi, 1965). Fault-slip data are collected from meso-scale faults in northern and central Ryukyu arc islands. The geology of the Ryukyu arc was summarized by Kizaki (1985, 1986). The stratigraphy of the northern and central Ryukyu arc islands is given in Figure 2.

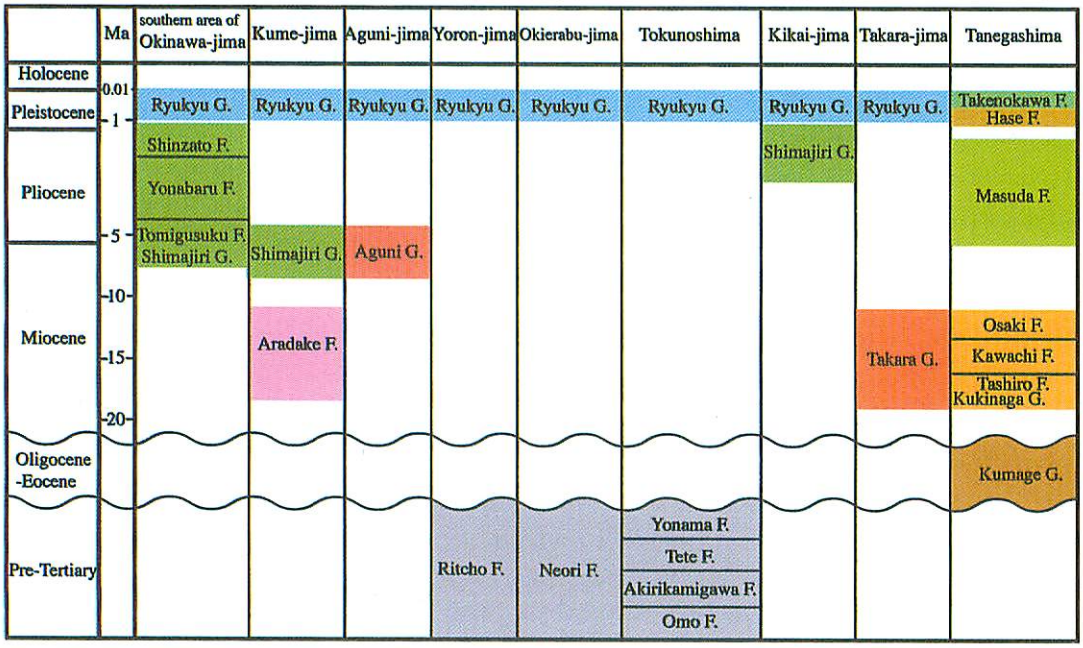

Fig.2. Stratigraphy of the northern and central Ryukyu islands (compiled from Kizaki (1985), Nakamori (1986) and Kizaki (1986)).

The paleomagnetic rotation of the Ryukyu arc has occurred in northern and southern part (Miki et al., 1990; Kodama et al., 1991; Kodama and Nakayama, 1993; Kodama et al., 1995; Miki, 1995). Kodama et al. (1995) suggested that the rotation of south Kyushu and northern Ryukyu arc occurred during the past 2 Ma. Between 6 and 10 Ma, the northern Ryukyu arc did not rotate (Kodama et al., 1991; Kodama and Nakayama, 1993) and the central Ryukyu arc did not experience any significant rotation (Miki, 1995). For the same 10-6 Ma period the southern Ryukyu arc rotated 25° clockwise (Miki et al., 1990; Miki, 1995).

2.1. Okinawa-jima

Okinawa-jima is the largest island in the Ryukyu arc, which is located in middle of the Ryukyu arc. Northern part of the Okinawa-jima is composed of pre-Neogene basement rocks. On the other hand, southern part of the Okinawa-jima consists of Neogene sediments; Shimajiri and Ryukyu groups. Shimajiri group is the basement of southern part of Okinawa-jima and mainly consists of mudstone interbedded by sandstone and tuff. The group is distributed in the forearc area on land and offshore along the Ryukyu islands (Kizaki, 1986). Ujiie (1994) performed micropaleontological study of the Shimajiri group in the Okinawa-jima, Miyako-jima and Kikai-jima. Hereafter this section is referred from the articles of Kizaki (1985), Kizaki (1986), Nakamori (1986) and Ujiie (1994).

The Shimajiri group is composed of bathyal sediments, and from the studies of microfossil, this group deposited from late Miocene to early Pleistocene (Ujiie, 1994). In general, this group dips about 10 - 20° and strikes NE trending. Shimajiri group is divided into three formations; Tomigusuku, Yonabaru, and Shinzato formation in ascending order.

The Tomigusuku formation distributes in the western part of the southern part of Okinawa-jima (Fig.4). Upper part of the formation called "Oroku Sandstone" is mainly composed of massive and yellowish sandstone and it exceptionally shows slumping structure. Lower part of the formation mainly consists of mudstone. It is difficult to find fault-slickenline in the Oroku sandstone because most of the fault plane within the sandstone is the close type.

The Yonabaru formation overlies conformably the Tomigusuku formation, and is widely exposed (Fig.5). The formation consists of grayish mudstone interbedded with thin sandstone and tuff. Tuff layers within this formation are useful for key beds. The total thickness of the formation is about 1400m. The Nakagusuku Sandstone member dominating the base of the formation consists of turbidite sands with about 3-8 m thickness in general. Slumping structures are observed in the Tomigusuku and Yoanabaru formations. Fault-slip data of the fault associated slumping structure are not collected, because outcrops of the slumping show complex structure.

The Shinzato formation conformably covers the Yonabaru formation. The formation is observed in small area, the Chinen Peninsula and the eastern small islands; Miyagi-jima and Hamahiga-jima (Fig.6). The lower part of the formation is called "Shinzato Tuff" whose thickness is 5 to 10 m. In contrast to the Yonabaru formation, sandstone becomes abundant.

The Ryukyu group rests unconformably on the Shimajiri group. The Ryukyu group composed of reef complex deposits, mainly limestone associated with sand and gravels. Many researchers have divided the Ryukyu group in the Okinawa-jima into several units (Flint et al., 1959; MacNeil, 1960; Takayasu, 1976; etc.). Age and stratigraphy of the Ryukyu group is described in this section where the most parts are referred from

Nakamori (1986) and Kaneko (1996).

The Ryukyu group in the Okinawa-jima is divided into three formations; Chinen, Naha and Minatogawa formation in ascending order (Nakamori, 1986). The Kunchan Gravel and Yontan Limestone are included in the Naha formation (Nakamori, 1986).

The Chinen formation called "Chinen Sand" is distributed in the limited area of southeastern part of the Okinawa-jima, the Chinen peninsula, and the eastern small islands, Hamahiga-jima, Henza-jima and Miyagi-jima. This formation consists of brownish calcareous sandstone and sandy limestone, which is weakly consolidated and yields many fossils. The Chinen formation is correlative with the transitional lithofacies between the Shimajiri group and Ryukyu group.

The Naha formation is the main part of the Ryukyu group in the Okinawa-jima. This formation is 50 m in maximum thickness.

Outcrops of the Minatogawa formation, named firstly Machinato formation by Flint (1959), called Minatogawa Limestone by Takayasu (1976, 1978) are seen in the quarry of southern part of the Okinawa-jima. Maximum thickness of the formation is 20 m which overlies the Naha formation or the Shimajiri group unconformably (Nakamori, 1986).

Age of Ryukyu group is estimated by some researchers using various method (Kizaki et al., 1984; Kawana, 1989; Sado et al., 1992; Kaneko and Ito, 1995; 1996; Ninagawa et al., 2000; Sato et al., 2004). The age of the lowest part of the group in Irabu-jima is estimated 1.2-1.3 Ma (Sado et al., 1992). Kaneko and Ito (1995) reported Sr isotopic composition of basal part of Ryukyu group called "Reddish Limestone" (Kaneko, 1994) in southern Okinawa-jima and estimated about 1.3 Ma. The age of the Chinen formation is reported based on calcareous microfossils by Sato et al (2004), which is estimated 2.09-1.65 Ma. The age of the Naha formation is estimated about 0.4 Ma by $^{87}Sr/^{86}Sr$ ratios (Kaneko and Ito, 1996) and the Minatogawa formation is dated as 0.12-0.13 Ma by compared to terrace (Kawana, 1988) and thermoluminescence method (Ninagawa et al., 2001).

Many active faults are recognized in the study area of the Okinawa-jima (Research group for Active Faults of Japan, 1991), and their result indicates that the area has active tectonic event after the deposition of Ryukyu group.

2.2. Aguni-jima

Aguni-jima is a small island which situated about 60 km northwest from Naha city in Okinawa-jima (Fig.7). The section hereafter is referred from the article of Kizaki (1985).

Aguni group is the basement in Aguni-jima. This group is composed of pyroclastic rocks, and divided into three formations; Nishi, Fudensaki and Higashi formation in ascending order. The Nishi formation mainly consists of dacite lava. The formation was dated as 6.24 ± 0.46 Ma using Fission Track method by Daishi (1987). The Fudensaki formation covers unconfomably Nishi formation and mainly consists of tuff. Higashi

formation is composed of alternated beds of lava and pyroclastic rock. The age of the Aguni group is considered from late Miocene to early Pliocene (Kizaki, 1985). Fault-slip data are collected from the Fudensaki formation.

Doji formation of Ryukyu group is exposed widely in the Aguni-jima. The detailed age of the Doji formation is not clear.

The major active fault running along NE-SW in the island is called "Aguni fault" (Furukawa, 1979; Research group for Active Faults of Japan, 1991). As the Aguni fault does not cut the coral reef terrace, the fault is assumed to be low activity and not active within the latest 10 Ka (Research group for Active Faults of Japan, 1991).

2.3. Kume-jima

Kume-jima lies about 90 km west from Naha city in the Okinawa-jima (Fig.8). The section hereafter is referred from the articles of Kizaki (1985), Nakamura et al. (1999) and Ehara (2001).

Aradake formation consists mainly of pyroclastic rocks, dated as 12-18 Ma (Nakagawa and Murakami, 1975; Daishi, 1987; Miki, 1995). Shimajiri group is divided into three formations; Maja, Aka and Uegusuku formation, in ascending order (Nakagawa and Murakami, 1975; Nakamura et al., 1999). From several methods, these formations are dated as 7.2-8.6 Ma, 2.6-3.2 Ma and 2.2 Ma, respectively (Ehara, 2001). Fault-slip data are sampled from mainly Maja formation. The Ryukyu group is divided into Nakandakari formation, Kumejima formation, Torishima formation, and Oha Limestone (Ehara, 2001). Ehara (2001) reported that the age of the Kumejima formation is about 1.57 Ma from nannofossil. However, the detailed age of the Ryukyu group is not clear. Fault-slip data are obtained from the Kumejima formation.

The major fault trending along ENE is called the Kume fault (Kizaki, 1985), while active faults are not recognized in this island (Research group for Active Faults of Japan, 1991).

2.4. Yoron-jima

Yoron-jima is the southernmost island of the Amami islands and it lies about 20 km north from the northernmost part of the Okinawa-jima (Fig.9). The section hereafter is referred from the articles of Kizaki (1985) and Odawara and Iryu (1999).

Basement of Yonaguni-jima is composed of pre-Tertiary rocks, which is named as Ritcho formation (Nakagawa, 1967). The Ryukyu group of the island is mainly consisted of limestone. Odawara and Iryu (1999) divided the Ryukyu group into five formations; Mugita, Ugachi, Yoronjima, Chichizaki and Tomori formation. The lowest Ugachi and Mugita formations consist of partly karstified coral limestone. The Yoronjima formation unconformably overlies the Ugachi and Mugita formations, which is exposed widely in this island. The Chichizaki and Tomori formations unconformably resting on the

Yoronjima formation are composed mainly of thin coral limestone. Fault-slip data are collected mainly from the Yoronjima formation.

On the basis of calcareous microfossils study, the Yoronjima formation is estimated 0.89-0.39 Ma (Odawara and Iryu, 1999). Compared with the unit of Ryukyu group in the Okinoerabu-jima and Tokunoshima, the age of the Yoronjima formation is estimated at least 410-950 Ka (Yamada et al., 2003).

NNW and WNW trending faults are active fault (Research group for Active Faults of Japan, 1991). Two active faults divide the Yoron-jima into three blocks.

2.5. Okinoerabu-jima

Okinoerabu-jima locating between the Tokunoshima and Yoron-jima, is the southern island of the Amami islands and lies about 60 km north from the northernmost part of the Okinawa-jima (Fig.10). The section hereafter is referred from the articles of Kizaki (1985) and Iryu et al. (1998).

The basement of the Okinoerabu-jima is composed of the Mesozoic sedimentary rocks, and Tertiary granodiorite and porphyrite, which is named as Neori formation (Nakagawa, 1967). The Ryukyu group mainly consists of limestone, which overlies unconformably the Neori formation. Iryu et al. (1998) divided the Ryukyu group into two units; lower and upper units. Fault-slip data are taken mainly from the lower unit.

En echelon active faults trending WNW are reported (Research group for Active Faults of Japan, 1991).

Although Ikeda et al. (1991) reported the electron spin resonance (ESR) ages ranging from 730 to 840 Ka for the lower unit of the Ryukyu group in the Okinoerabu-jima, the age of the Ryukyu group is not well constrained and it is adequate to say that the age of the group ranges widely from ca. 400 to 900 Ka (Iryu et al., 1998).

2.6. Tokunoshima

Tokunoshima is the second large island in the Amami islands and lies about 30 km north from the Okinoerabu-jima. Tokunoshima is the sixth large island in the Ryukyu arc and have the second highest peak in the Amami islands. The section hereafter is referred from the articles of Kizaki (1985), Iryu et al. (1998) and Yamada et al. (2003).

The basement of the Tokunoshima is composed of the Mesozoic sedimentary rocks and the Tertiary granitic rocks. The basement is divided into four formations; Omo, Akirikamigawa, Tete and Yonama formation (Nakagawa, 1967). Boundaries of each formation are considered to cut by faults.

The Ryukyu group, which is mainly composed of limestone overlies unconformably the basement. The Ryukyu group have comprised two formations; Tokunoshima formation and Metegu formation (Yamada et al., 2003). The Tokunoshima formation is divided into two units. Fault-slip data are collected from mainly unit 1 of Tokunoshima formation.

Several researchers (Koba and Nakata, 1981; Omura, 1982; Iryu and Yamada, 1991) reported the age of the Ryukyu group in the Tokunoshima. The age of Tokunoshima formation is dated 0.41-1.65 Ma from the data of nannofossil (Yamada et al., 2003). In unit 1 of the Tokunoshima formation, Omura (1982) reported the ages of >300 Ka by $^{230}Th/^{234}U$ method and 387-709 Ka by $^{234}U/^{238}U$ method. Iryu and Yamada (1991) reported 481 17 Ka at the same sample point by ESR method. After considering all the available data, it is concluded that the Tokunoshima formation has started its deposition before about 0.48 Ma (Yamada et al. 2003). Although Koba and Nakata (1981) detected the age of the Ryukyu group ranging from 146 to 290 Ka by ESR method, this ESR age is assumed the youngest age. An ESR date denotes that the Metegu formation was accumulated at >146 Ka (Yamada et al., 2003).

Major faults cutting the Ryukyu group are called Inutabu, Isenzaki and Hetono Fault. These are active faults (Research group for Active Faults of Japan, 1991), which are activated after deposition of the Tokunoshima formation (Yamada et al., 2003).

2.7. Kikai-jima

Kikai-jima is a small island, which is located in the eastern part of the Ryukyu arc and lies about 20 km east from the Amami-oshima. The section hereafter is referred from the articles of Kizaki (1985) and Ujiie (1994).

The geology of Kikai-jima consists of two groups (Shimajiri group and Ryukyu group) and Holocene deposits. The Shimajiri group called Soumachi formation (Nakagawa, 1969) is the basement, which consists of mainly mudstone and sandstone. The deposition of the formation is dated in the late Pliocene to earliest Pleistocene by planktonic foraminiferal studies.

The Ryukyu group is composed of Hyakunodai and Wan formation, which unconformably covers the Somachi formation. Several researchers (Omura, 1988; Ikeda et al., 1991; etc.) have estimated the age of the Ryukyu group in the Kikai-jima. Ikeda et al. (1991) detected the age of the Ryukyu group ranging from the 570 to 650 Ka by ESR method.

2.8. Takara-jima

Takara-jima is a small island, which is located in the volcanic front of the Ryukyu arc and lies 86 km northwest from Naze city in the Amami-oshima. Takara-jima and Kodakara-jima are northern limit of coral islands in the western pacific (Hirata, 1967). A kind of venomous snake, *Trimeresurus favoviridis tokarensis NAGAI,* inhabits only these two islands. The section hereafter is referred from the article of Kizaki (1985).

The geology of Takara-jima is divided into two groups; Takarajima group and Ryukyu group (Kizaki, 1985). The Takarajima group is composed of pyroclastic rocks. Age of the Takarajima group is detected as Miocene by comparing with the activity of Green

tuff in south Kyushu (Matsumoto, 1983). The Ryukyu group is divided into Ooma conglomerate layer, Ryukyu limestone, Kan-non sandstone and conglomerate layer. Fault-slip data are collected from the Ryukyu limestone.

2.9. Tanegashima (northern Ryukyu arc)

Tanegashima lies about 40 km south from the southernmost part of Kyushu. The section hereafter is referred from the article of Kizaki (1985).

The basement in this island, Kumage group, belonging to the Shimanto accretionary complex, consists of the Eocene to Oligocene strata. The Kumage group is exposed in the northern and southeastern part of the Tanegashima and has been deformed by intense folding and faulting. Due to the very complex structure, fault-slip data have not been collected from this group. The Kumage group is divided into four formations; Nijuban, Hamatsuwaki, Fukagou and Sumiyoshi formation, respectively (Kizaki, 1985).

The Kukinaga group in the southeastern part of Tanegashima, overlies on the Kumage group, which is the middle Miocene marine sediment. The Kukinaga group, which has moderately tilted, is less deformed than the Kumage group. Fault-slip data are collected from the Kukinaga group. The Kukinaga group is divided into three formations; Tashiro, Kawachi, and Osaki formation in ascending order. The age of the Kukinaga group is determined the middle Miocene by marine fauna included in the Kawachi and Osaki formation (Hayasaka, 1969). The youngest age for the Kukinaga group has been proposed as 16 to 10 Ma from based on the macrofossil and microfossil evidence (Kodama et al., 1991).

The Tashiro formation consists of mainly conglomerate with some sandstone and mudstone strata and rarely coal but not continuity. The formation has bad-sorted round gravel in general.

The Kawachi formation, which is mainly composed of grayish mudstone with thin sandstone and conglomerate, overlies conformably the Tashiro formation. This formation yields many fossils (coastal and embayment type).

The Osaki formation, which consists of mainly well-sorted yellowish sandstone with thin conglomerate and mudstone layers, overlies conformably the Kawachi formation. The formation shows good exposures. Many fault-slip data are collected from this formation. The formation yields different type fossils (oceanic shallow type). Cross lamina are developed in several localities of the formation.

The Masuda formation covers unconformably the Kukinaga group. Age of the formation is Pliocene from the marine invertebrate fossil study (Hayasaka, 1973). The formation consists of mainly sandstone.

The Hase formation is seen as about 3-5 m gravel layer, which is covered by volcanic ash unconformably. The Takenokawa formation is the marine sediment, which consists of mudstone, sandstone and conglomerate. The thickness of the formation is

about 10 m. Age of Hase and Takenokawa formation is detected as Pleistocene (Kizaki, 1985).

3. Method of fault-striation analysis

Paleostress field are detected by the fault striation analysis (Multiple inverse method and Ginkgo method). Fault-slip data of meso-scale fault are measured that is a fault which can be seen in the outcrop scale (Angelier, 1994). The fault-slip data are composed of the strike and dip of faults, and trend and plunge of slickenlines on the fault plane. Stress history of the Ryukyu arc is detected by the fault-slip data.

3.1. Multi-inverse method

The Multi-inverse method (Yamaji, 2000) is a numerical technique to separate stresses from heterogeneous fault-slip data. The method is an extension of classic inverse method developed by Angelier (1979). This section hereafter is referred from Yamaji (2000).

Multi-inverse method is based that inversion is applied to a number of ${}_{N}C_{k}$ subset data where is binomial coefficient to detect more stress from heterogeneous data. The choise of a value for k is arbitrary. Optimal stress is represented by cluster of solution applied to number of ${}_{N}C_{k}$ subset data.

$$ {}_{N}C_{k} = \frac{N!}{k!(N-k)!} $$

Significant stress states for a given data set are represented by the clusters of symbols like tadpoles on the stereograms. The color of the symbols indicates the stress ratio. Stress rario ϕ is described by following equation.

$$ \phi = \frac{\sigma_2 - \sigma_3}{\sigma_1 - \sigma_3} $$

The end members, violet and red, indicate the stress states that are symmetric with respect to σ_1 and σ_3 axes, respectively. It should be noted that an axial stress is designated not only by a cluster but also a great-circle girdle whose pole is parallel to the symmetric axis (Yamaji et al., 2003).

3.2. Ginkgo method

The Ginkgo method is also the numerical technique to detect plaeostress from fault-slip data (Yamaji, 2003a). The section hereafter is referred from Yamaji (2003a). The Multi-inverse method requires many data in order to separate stresses from heterogeneous assemblage. The Ginkgo method is useful to calculate in the case where fault-slip data is few (N<10). For fault striation analysis, four parameters (angle of three principal stress axes and stress ratio) can be found from fault-slip data. Therefore, one can consider these

parameters as one function F. the programs of Ginkgo method is composed of main and post processor. The main processor calculates the fit, F, at all grid points and tabulates the results with the direction of stress axes and stress ratio arranged in the ascending order of F. The post processor represents the table using a couple of color stereograms: both are lower hemisphere equal area plots, and the left and right stereograms always indicate the direction of σ_1 and σ_3 axes, respectively. Φ and F are indicated by hue and saturation of color, respectively. Color saturation is a degree to which a pure color of the spectrum is diluted by white. Only the relative value of the F is meaningful, so that the relative fit, defined as F minus the minimum F, is represented by color saturation. High and low relative fits are indicated by pure and whitish colors, respectively.

The parameter space is four-dimensional, so that stereographic projection involves the reduction of information. Specifically, many points with the same σ_3 direction but different σ_1 directions are projected on the same point among those. To minimize the overlapping projection, the plotted points were dispersed around the points within a radius of 8°. Consequently, the stereograms are filled with dots with various colors, although the fit is calculated at discrete grid points. The color plotting is executed in the ascending order of F, so that the color dots with lower F are hidden by those with higher F.

4. Fault-slip data

Fault-slip data are collected from the northern and central Ryukyu arc; Okinawa-jima, Kume-jima, Aguni-jima, Yoron-jima, Okinoerabu-jima, Tokunoshima, Kikai-jima, Takara-jima and Tanegashima. Table 1-12 show these fault-slip data.

Table 1. Meso-scale faults measured from the Tomigusuku formation in the Okinawa-jima. In slickenline data, trend and plunge are described. Sense data indicate fault type. N: normal fault, R: reverse fault, D: dextral strike-slip fault, and S: sinistral strike-slip fault.

Unit	Fault plane	Slickenline	Sense
OTo1	N37E80W	N47W80	N
OTo2	N82E63W	N83W21	N
	N26W80E	N65E80E	N
OTo3	N44W59E	N76E47	N
	N45E65W	N38W64W	N
	N63W78W	N24E78	R
	N75W70E	N28E65	N
	N65W65E	N21E63	N
	N70W72E	N31E68	N
	N57E62W	N43W62	N

	Unit	Fault plane	Slickenline	Sense
OTo4		N76E65W	N25W58	N
		N37E78W	N58W73	N
	Shimajiri.G	N52E72W	N40W72	N
	Tomigusuku F.	N39E64W	N64W57	N
		N15W90	N68E76W	N
OTo5		N85W77E	N6E77E	N
		N47W45W	S47W45	N
		N44W80E	N60E78	N
		N39W62W	S33W51	N
OTo6		N2E66W	N82W63	N
		N14E59E	N33E28	N
		N80E73W	N12W71	N
		N33E20E	S89W20E	R
		N41W81W	S50W79	N
		N32W38W	S18W25	N
OTo7		N59W58W	S22W53W	N
OTo8		N88W67E	S15E67	R
		N53E57W	N43W57	N

Table 2. Meso-scale faults measured from the Yonabaru formation in the Okinawa-jima. Data format is same as Table 1.

	Unit	Fault plane	Slickenline	Sense
OYo1		N41W62W	S22W38	N
		N45W75W	S54W56	N
		N23E75W	S82W75	N
		N43E88W	N49W87W	N
		N51E55W	N57W53W	N
		N22E52W	N58W52	N
		N33E61W	N60W58	N
		N42E57W	N50W57	N
		N23E53W	N68W53	N
		N11E45W	N74W45	N

	Unit	Fault plane	Slickenline	Sense
OYo2		N25E75E	S54E65	N
		N11E64W	N72W64	N
		N8W45E	N78E40	N
		N3W67W	S90W60	N
		N50E57E	S74E40	N
		N6E52W	N82W51	N
OYo3		N72E56W	N10W48	N
		N80E56W	N8W56	N
OYo4	Shimajiri.G	N28E59W	N73W59	N
	Yonabaru F.	N2W50W	S69W45	N
		N8E57W	S85W57	N
		N11E56W	N86W52	N
OYo5		N11W70W	N68E69	N
		N22W68W	S74W65	N
		N82E59W	N0E58	N
		N5E62W	N85W61W	N
		N82W62W	S24W57	N
		N17E60W	N75W59	N
		N4E52W	S88W51	N
		N3E61W	N82W60W	N
		N34E68W	N58W60	N
		N27E63W	N64W63	N
		N19E55W	N51W54	N
		N31E68W	N69W62	N
		N7E60W	N84W58W	N
		N11E65W	N68W61	N
		N13E63W	N78W61W	N
		N52E62W	N47W62	N
		N76E63W	N18W58W	N
		N56E58W	N32W55W	N
		N46E72W	N46W70W	N
		N5E57W	S82W57	N
		N2W58W	S81W57	N
		N2E66W	S84W62	N
		N60E51W	N32W47	N
		N79E49W	N10W49	N

	Unit	Fault plane	Slickenline	Sense
OYo5		N60E58W	N26W54	N
		N37E69W	N50W69	N
		N42E66W	N48W65	N
		N37E59W	N46W59	N
	Shimajiri.G	N56E54W	N22W54	N
	Yonabaru F.	N22E68W	N57W68	N
		N11E63W	N83W60	N
		N33E69W	N65W65	N
		N54E43W	N43W43	N
		N17E67W	N80W67	N
		N3W64W	N78W64	N
		N60E51W	N30W50	N
		N75E38W	N38W34W	N
		N38E73W	N44W73	N
		N55E49W	N33W47	N
		N15E52W	R85E	N
		N12E57W	R78E	N
		N30E77W	R87E	N
		N56E50W	R89E	N
		N61E47W	R80E	N
		N5E48W	R88E	N
		N37E44W	R90E	N
		N10W65W	R69W	N
		N5E61W	R83E	N
		N7E62W	R90E	N
		N37E62W	R82E	N
		N49E61W	R79E	N
	Shimajiri.G	N5E69W	R78E	N
	Yonabaru F.	N54E51W	R90E	N
		N57E61W	R86E	N
		N7E72W	R85W	N
OYo6		N38E80W	N52W77W	N
		N41E50E	S54E49E	N
		N62E70W	N29W70W	N
		N41E65W	N60W55W	N
		N38E67W	N57W67W	N
		N32E64W	N46W60W	N

	Unit	Fault plane	Slickenline	Sense
OYo7		N28W43E	N42E35	N
OYo8		N37E43E	S32E41	N
		N17E73E	S82E70	N
		N3E70E	S78E69	N
		N56E50E	S35E50	N
		N45E58W	N43W58	N
		N62E49E	S24E44	N
		N63E72W	N17W72	N
OYo9		N67E50W	N38W49	N
		N63E48W	N22W48	N
		N83E47W	N7E46	N
OYo10		N72E58W	S6W56	R
OYo11		N46E71W	N37W71	N
		N15E82W	N83W82	N
OYo12		N44E54W	N44W48W	N
OYo13		N54W70E	N16E68	N
		N10W72W	S84W70	N
OYo14		N76W82E	N2W82	N
		N83E78E	S23E70E	N
		N86E67W	N6E64W	N
		N81E80E	S7E80E	N
		N36E60E	N53W60	N
		N84E65W	N15W60	N
OYo15	Shimajiri.G	N14W62E	N66E62	N
	Yonabaru F.	N22E70E	N75E70	N
		N31W68E	N63E68	N
		N24W58E	N62E57	N
		N51E64W	N38W63	N
		N63E65E	S25E65	N
		N53E72W	N29W68	N
		N53E68W	N38W66	N
		N58E72E	S20E72	N

Table 3. Meso-scale faults measured from the Shinzato formation in the Okinawa-jima. Data format is same as Table 1.

	Unit	Fault plane	Slickenline	Sense
OShi1		N16E82E	N56W80E	N
		N15E48W	N67W46W	N
		N9E75E	S86E73	N
		N18E81E	S67E77	N
		N13E87E	S74E85	N
		NI6E75E	S82E72	N
		N15E88E	S86E72	N
		N10E83E	S82E83	N
		N12E88E	S76E86	N
OShi2		N88W83E	N9W73E	R
		N62E8lW	N32W73	R
		N80E78W	N21W72	N
		N79E77W	N17W75	N
		N77E88W	N24W85	N
		N67E78W	N15W69W	N
OShi3	Shimajiri.G	N60E78E	S38E78	N
	Shinzato F.	N39E65W	N42W60	N
		N65E79W	N40W70	N
OShi4		N8773E	N8E73	N
		N86W6lE	N3E58	N
		N87E68W	Nl2E68	N
		N81E78E	N4W78	N
		N88E53W	N7E53W	N
		N87E63E	Sl2E6IE	N
		N74W88E	Nl5E87	N
		N30W85W	S56W8l	N
		N26W88W	S6lW84E	N
		N7778W	R8lE	N
		N69W8W	R87E	N
		N89W65W	R84E	N
		N58W69E	R80E	N
		N89W70W	R83E	N
OShi5		N13W58E	N90E58	N

Table 4. Meso-scale faults measured from the Ryukyu group in the Okinawa-jima. Data format is same as Table 1.

Unit	Fault plane	Slickenline	Sense
OR1	N54E64NW	R62W	N
	N10E60W	R68W	N
OR2	N26E69W	R87E	N
	N81W6IE	R62E	N
	N72W73E	R74E	N
	N51W80E	R72E	N
	N26W79E	R69W	N
OR3	N54W70W	R76E	N
	N20W84W	R75W	N
	N87E80W	R75E	N
	N88W67W	R80E	N
OR4	N38E71W	R74E	N
	N23W77E	R71E	N
	N35E63E	R60E	N
	N3E78E	R57W	N
Ryukyu Group	N35W46E	R70W	N
	N29W65E	R83W	N
	N6W73E	R72W	N
	N52E66W	R83W	N
OR5	N34W67W	R76E	N
	N9E70W	R79W	N
	N7E65E	R81W	N
	N24E85W	R55E	N
	N36E83E	R75E	N
	N2E80W	R76W	R
	N29E80W	R70W	N
	N45E58W	R77E	N
	N16E72W	R62E	N
	N4W62W	R80E	N
	N45W84E	R83E	N
	N52W53E	R71W	N
OR6	Ni1W71W	R82W	N
	N41E70W	R88W	N
	N80E83E	R79W	N
OR7	N25W77E	R65E	N
	N65W82E	R67E	N

Table 5. Meso-scale faults measured in the Aguni-jima. Data format is same as Table 1.

	Unit	Fault plane	Slickenline	Sense
AA1		N42W55E	R78E	N
		Nl9W63W	R75W	N
		N40W55E	R67E	N
		Nl5W74E	R68W	N
		NS77W	R73S	N
		N30W60W	R76W	N
AA2	Ryukyu Group	N62W69W	R68E	N
		N79W71W	R68W	N
		N24W58W	R75W	N
		N62W74W	R84W	R
		N61W7Y	R74E	N
AA3		N77W55W	R69W	N
AR1		N20E74W	R76W	N
		N33E74W	R67E	N
		N50E63W	R78W	N
		N55E74W	R78E	N
		N52E64W	R74W	N
	Aguni Group	N23E62W	R76E	N
AR2		N20W8IE	R86E	N
		N20E52E	R87W	N
		N4lW72E	R58E	N
		N133W70E	R78E	N
		N49W71E	R46W	N
		NI0E68E	R70W	N

Table 6. Meso-scale faults measured in the Kume-jima. Data format is same as Table 1.

	Unit	Fault plane	Slickenline	Sense
KuR1		N77W66W	R80W	
KuR2		N15W63E	R65E	
		N10E81E	R75W	
KuR3	Ryukyu Group	N48W38W	R82E	
		N8774W	R70E	
		N74W76E	R69E	
KuR4		N86E87W	R72W	
		N41W87W	R76E	
KuR5		N45W84W	R59W	
KuS1		N47W61E	N47E57	
KuS2		N62E78E	S57W62	
		N35W79W	N56E73	
KuS3		N53W58E	N46E53	
KuS4		N44E63E	S56E56	
		N12W47E	N88E44	
		N53E83E	N35W83E	
		N30E80W	N67W80	
		N28E71W	N70W78	
KuS5		N84E47W	N34W20	
		N63W45E	N26E49	
KuS6		N87W72E	N2E76	
KuS7	Shimajiri Group	N72E86W	N19W74	
KuS8		N15E22W	S75W16	
KuS9		N40W87E	N59E78	
		N31W83E	N74E75E	
		N35W82E	N53E85	
KuS10		N37E64E	S60E59E	
		N3IE53E	S68E53E	
		N23E83W	N70W75W	
KuS11		N26E36E	N76W30E	
KuS12		N81W84E	N6E80	
		N82E87	N2W78	
KuS13		N46W88E	N53E35	
		N10E59W	N83W59	
		N85W30E	N20W26	

Table 7. Meso-scale faults measured in the Yoron-jima. Data format is same as Table 1.

Unit		Fault plane	Slickenline	Sense
YoR1		N57E44E	R86E	N
		N38W70E	R64E	N
		N37W82E	R73E	N
		N22E80E	R58W	N
		N48W71E	R65W	N
		N30E77E	R82W	N
		N61W72E	R57E	N
		N47E50W	R71W	N
		N80E86E	R82W	N
		N81E77W	R75W	R
		N29W75E	R73E	N
YoR2		N16E71W	R67E	N
		N63W58W	R70W	R
		N28E85E	R75E	N
		N77W84W	R71E	N
		N26E61E	R64E	N
		N76E87E	R89E	N
		N59E80E	R68E	N
	Ryukyu Group	N12W69E	R80E	N
YoR3		N49W75W	N81E67W	N
		N58E75W	R71W	N
YoR4		N82W75W	R70W	N
		N53W60W	R62W	N
		N82E87E	R63W	N
		N36W72W	R75E	N
		N60E73E	R60E	N
		N10E68E	R70W	N
YoR5		N54E84E	R74E	N
		N51E55W	R78E	N
		N78W46E	R65W	N
YoR6		N32E6E	R78E	N
YoR7		N74W78E	R71W	N
		N40E61E	R81E	N
		N11W80E	R76W	N
		N50W53W	R78E	N
		N18W77W	R60W	N
YoR8		N82E60W	R85E	N
		N84W66E	R87W	N
		N58W58E	R79W	N

Table 8. Meso-scale faults measured in the Okinoerabu-jima. Data format is same as Table 1.

	Unit	Fault plane	Slickenline	Sense
OeR1		N21E88E	R78W	N
		N80E85W	R77E	N
		N53E73W	R70W	N
		N72E69W	R71E	N
		N68E79W	R78E	N
		N16W80E	R60W	N
	Ryukyu Group	N84W69E	R36W	N
OeR2		N69W79E	R76W	N
OeR3		N72E71E	R75W	N
		N65E85E	R72W	N
		N84W70W	R64E	N
OeR4		N77E70W	R80E	N
		N66E67E	R8IW	N
		N8lE82W	R80E	N
		N39E77E	R69E	N

Table 9. Meso-scale faults measured in the Tokunoshima. Data format is same as Table 1.

	Unit	Fault plane	Slickenline	Sense
ToR1		N49W82W	R78E	N
		N84W79W	R82E	N
ToR2		N59W78W	R83E	N
		N38W70W	R87E	N
		N56W81E	R56W	N
		N55W85W	R61E	N
		N62W80E	R80W	N
		N55W79E	R69W	N
		N66W60W	R57W	N
		N37W77E	R51W	N
		N4E86E	R58E	N

	Unit	Fault plane	Slickenline	Sense
ToR3		N22W73E	R79E	N
		N56W75E	R46W	N
		N51E80E	R64W	N
		N50E75E	R72E	N
		N77E75W	R55E	R
	Ryukyu Group	N82W71E	R64W	R
		N47W61E	R72W	N
ToR4		N1W52W	R77W	N
		N12E71W	R75E	N
		N26W46W	R70E	N
		N28W41W	R62W	N
		N72E59W	R78W	N
ToR5		N87W85E	R52E	D
		N11E80E	R52W	D
		N77W74W	R83E	N
		N45W76W	R80W	N
		N54W79E	R80E	N
		N54W68E	R70E	N
ToR6		N25E59W	R88W	N
		N37W43E	R77E	R
		N20W77W	R79W	N
		N48W82E	R67W	N
		N33W84W	R67W	N
		N38W83W	R56W	R

Table 10. Meso-scale faults measured in the Kikai-jima. Data format is same as Table 1.

	Unit	Fault plane	Slickenline	Sense
KiR1		N24W80W	R62W	N
		N19W67W	R43W	N
		N59W71E	R67W	N
		N87W79W	R81E	R
		N50W63E	R73W	N
	Ryukyu Group	N37E80W	R80W	N
		N26W64W	R74E	N
		N74W64W	R56W	N
		N59W83W	R65E	N
KiR2		N23W34W	R77E	N
		N33E83E	R85W	N

	Unit	Fault plane	Slickenline	Sense
KiS1		N52E52E	S30E52	N
		N30E58E	N88E53	N
		N80E29E	S13E29	N
KiS2		N14W52W	S49W52	N
		N72E67W	N10W59	N
		N38E63W	N63W62	N
		N23E88E	S68E82	N
		N51E63E	S25E59	N
		N38E56E	S32E56	N
		N24E66W	N63W63	N
		N46E61W	N43W61	N
		N40E80E	S45E73	N
		N6E85W	R77W	R
		N34E53E	R70W	N
KiS3		N57E85W	N33W87	N
		N18E83E	S72E79	N
KiS4		N49E51W	N61W52	N
		N61E59W	N51W60	N
KiS5		N32E72W	R83W	R
		N14E86W	R70E	R

Table 11. Meso-scale faults measured in the Takara-jima. Data format is same as Table 1.

	Unit	Fault plane	Slickenline	Sense
TkT1	Takarajima Group	N80W85E	R71E	N
		N82E45W	R81E	N
TkR1		N4W81E	R73E	N
		N37E68E	R77W	R
		N29E78W	R66E	R
TkR2		N82W61W	R68E	N
	Ryukyu Group	N82W68E	R64W	N
		N67W63W	R67E	N
		N64E69E	R77E	N
		N19W66E	R54E	N
		N35E57E	R71W	R
		N58W81E	R80E	N
		N82W38E	R70W	N

Table 12. Meso-scale faults data measured in the Tanegashima. Data format is the same as Table 1.

	Unit	Fault plane	Slickenline	Sense
TA1	Takenokawa F.	N56W67E	R58E	N
TM1		N34W78E	N37E72	N
		N25W65W	S79W50	N
		N33W58W	N75W5l	N
TM2		N24W48W	R84E	N
		N22W48W	R88E	N
		N23W74W	R86W	N
	Masuda F.	Nl9W68W	R82E	N
		N25W73E	R88W	N
		N26W50W	R78W	N
		N32W72W	R77E	N
		N20W8lW	R64E	N
		N2lW68E	R8IE	N
		Nl8W77W	R60E	N
		Nl7W63W	R82E	N
		N20W73W	R6lE	N
TO1		N2lE54E	N54E35	N
		N70W81W	S70W79	N
		N9E53E	N88E52	N
	Osaki F.	N7E61E	N69E50	N
		N17E53E	N62E41	N
		N56W63E	R85W	N
		N57W31E	S23W29	R
		N74W36E	S12W35	R
TO2		N5E60W	S57W58	N
		N6E77E	N72E74	N
		Nl5W84W	S4E68	N
		N63W8lW	S70W74	N
		N73W87E	N24E87	N
		N27W65E	N34E62	N
		N25E77W	N80W76	N
		N7W87W	S46W75	N
		N9W60E	N87E60	N
		Nl2W63E	N77W60	N
		NIIW55E	N78W55	N
		N74W67W	N77E41	R
		N20W64E	N73E63	N

	Unit	Fault plane	Slickenline	Sense
TO3		Nl8W85E	Sl5W67	R
		N773E	N29W67	R
		N13W64E	N20E60	N
	Osaki F.	N6lW77E	N59E72	N
		N1781W	S8W59	N
		N43W83W	S8E57	N
		N6E77	S56W76	N
		N23W79W	S83W75	N
		Nl8W65W	N84W65	N
		N13W55W	N80W38	N
		N2E75W	S58W60	N
		NllW68E	N59E63	N
		N775W	S85W75	N
		N2E76E	N54E72	N
		N9W80E	N80E80	N
		N14W73W	S87W67	N
		N9W79W	S27W60	N
		N4lW53W	S37W51	N
		N42W55W	S21W52	N
		N9W84E	N53E83	N
		N2IE82E	N88E81	N
		N48W60W	S46W58	N
		N40W67W	N19E62W	N
		N48W78W	N8E78W	R
		N32W76E	N23E57	N
		N26E75E	N66E59	N
		N22E82E	N27W73	R
		N31E68E	S61E67	N
		N23E87E	N39W84	R
		N33E63E	N80E57	N
		N23E82E	Nl4E46	R
		N67E71E	S39E68	N
		N45E88E	N84W86	R
		N40E84E	S44E83	N
		N46E88E	S74W75	R
		N48E73E	S86W6l	R
		N8W82E	N67W80	R
		N49E82W	N6W78	N
		Nl9W75E	N63E67	N

Unit	Fault plane	Slickenline	Sense
TO3	N14W83W	S24W49	N
	N66E78W	N17E78	N
	N12W72E	S59E65	N
	N20W79E	N82E79	N
	N13W78W	N62W73	N
	N34W62E	N71E62	N
	N24W69E	S71E61	N
	N13W73E	N61E73	N
	N59W71W	S2E65	N
	N71W73E	N20E73	N
	N68W69W	S0E65W	N
	N64W82W	N15W72	R
	N16W75W	N87W74	N
	N70W61W	S17W58	N
	N46W70W	S80W63	N
	N48W81W	S84E76	R
	N11W71E	S33E56	N
	N30W58E	N88W47	N
TO4	N57W65E	N61E56	N
	N65W74E	N12W74	N
	N69W61E	N57E55	N
	N71W71E	N80E63	N
	N72W43E	N16W43	N
	N88W65E	N35E65	N
	N36E81E	N78E59	N
	N45E83E	N71W78	R
	N67W62E	N14E62	N
TO5	N84W88E	N20W86	N
	N30E81W	N61W81S	N
	N84E87W	S13E87	R
	N83E49W	N27W48	N
	N65E82W	N74W76	N
	N54E88W	N83W83	N
	N54E86W	N9E74W	N
	N20E82W	S7E69	R
	N12E77W	N42W70	N
	N53W82W	S10E70	N
Osaki F.	N56W88E	N24W80	N
	N40W88E	S18E67	R

Unit	Fault plane	Slickenline	Sense
TO5	N61W88E	N8W74	N
	N83W80E	S36E58	R
TO6	N62E86W	N25W80	N
	N57E88W	N33E69	N
TO7	N34W82E	N16E73	N
	N4E45E	N66E45	N
	N36W82E	N17E76	N
	N7E75W	S70W60	N
	N13W89E	S64E83	N
	N31W87W	N27E77	R
	N2W85E	N22E63	N
	N29E89W	N13E80	N
	N20W80W	S38E80	R
	N38E68E	N83W62	R
	N14W85E	N58E85	N
	N10W82W	S48W82	N
	N20W83E	S63W74	R
	N13W42W	S45W41	N
	N18E65E	S51E62	N
	N50W88W	S32W88	N
	N56W89E	N27E89	N
	N20W80W	N15E75	R
	N23W77W	S72E74	R
TO8	N18E79W	N34W66	N
	N20E77W	S63W77	N
	N61W78E	S61W66	R
TO9	21W41W	S64W40	N
	N25W46W	S72W46	N
	N9W54W	S63W42	N
	N9W73W	S40E73	R
	N15W42W	S89W36	N
	N12E79W	S84W77	N
	N12W88E	N47E84	N
	N16W50W	S87W50	N
	N17W60W	N65W53	N
	N11W53W	S78W44	N
	N43W87E	S46W83	R
	N25W56W	S56W48	N
	N22W77E	S63E72	N

Unit	Fault plane	Slickenline	Sense
TO9	N17W72E	N68E70	N
	N18W43W	N76W40	N
	N17W41W	S84W41	N
TO10	N79W58W	S0W53	S
	N10W79E	S2W37	R
	N1E87E	S37W84	R
TO11	N61W88W	R84E	R
	N7W30W	R84E	N
	N16W47W	R67E	N
	N33W85W	R81E	R
TO12	N25W75W	N52E75W	R
	N30W88W	N70E88	R
	N12W83E	S75E83	N
	N27W78W	S84W77	N
	N23W62W	S29W60	N
	N3E74W	N44W69W	N
	N64E63W	S62E63	R
	N87E76W	S61E46	R
	N56E69W	N46W60	N
	N21W86E	S50E73	N
	N30W87E	S64E76	N
	N21W77E	S20W73	R
	N47W71E	S60W71	R
TO13	N4W70W	N42E60	R
	N5E47W	N78W47	N
	N17W88E	N32E78	N
	N18W39W	N64W38	N
TO14	N88W70W	N11W69	R
	N18W80E	S55E67	N
	N3E78W	N67W78	N
	N4W62E	S80E61	N
	N14W87E	N52W62	R
	N44W86E	N70W74	R
	N21W78W	S54W70	N
	N10E61E	S81E61	N
	N2W75E	N65W70	R
	N1777E	N43E73	N
	N17E79E	S28E60	N
	N18W82E	S34E45	N
	N7E77	S27E	R
	N10W83W	N41W72	N

(A)

(B)

Fig.3. Photograph of the fault and slickenside in investigated islands. (A) Strike slip fault in the Ryukyu group (limestone), Takara-jima (TkR 1, in Fig.14). (B) Slickenside observed in the Ryukyu group, Okinoerabu-jima (OeR 4, in Fig.11).

Otsubo and Hayashi (2003) reported fault slicken line on the fault plane in the Ryukyu group and performed paleostress analysis. In the same way, Fault-slip data are measured from the Ryukyu group. Figure 3 shows the photograph of slickenside of a fault in the Ryukyu group. The fault of Ryukyu group is difficult to get fault-slip data because this group is composed mainly of limestone called "Ryukyu Limestone". The problems of Ryukyu limestone for fault analysis are; (1) recognition of key bed, (2) difficulty of the digging fault plane, and (3) identification of fault gap. In this study, fault-slip data are collected in the case where the fault has key bed and gap. Detailed observing the difference of the lamina, basement and coral in the Ryukyu group makes it possible to collect fault-slip data in this group.

With respect to grouping of fault-slip data, in order to estimate temporal change in fault activity, the criterion of the grouping was the stratigraphic units.

Fault-slip data are described in lower-hemisphere of equal-area projection. Two colors of blue and red indicate sense of the meso-scale fault. Normal fault type is blue and reverse fault type is red (Fig.4 - 15).

4.1. Okinawa-jima

Fault-slip data are collected from the Shimajiri and Ryukyu group. The site map and fault-slip data of both groups are shown in Fig. 4 - 7, respectively. More than 200 faults are observed in Okinawa-jima.

With regard to the fault in the Shimajiri group, some researchers (Etou, 1978; Ujiie, 1994) reproted the existence of many meso-scale faults of the normal type, while we have measured not only normal faults but also reverse faults.

4.1.1. Tomigusuku formation

The fault-slip data and the site map of the Tomigusuku formation are shown in Fig. 4. 26 fault-slip data are collected from this formation, which are grouped into three data sets; OTo1, OTo2 and OTo3. Fault data are grouped into one unit for each ca. 5 km square. Sense of the collected fault-slip data is almost the normal fault type, while there are also several reverse faults.

With regard to Oroku Sandstone, although there are many faults in the sandstone formation, fault-slip data are not obtained. It is difficult to obtain the fault-striation data because the sandstone is so weakly consolidated that one cannot excavate its slickenside striations.

4.1.2.Yonabaru formation

Figure 5 shows fault-slip data and their site map. 116 fault-slip data are obtained from the Yonabaru formation, because the formation is exposed wider area than the others. The fault-slip data are grouped into five data sets; OYo1 to OYo5. Fault data are

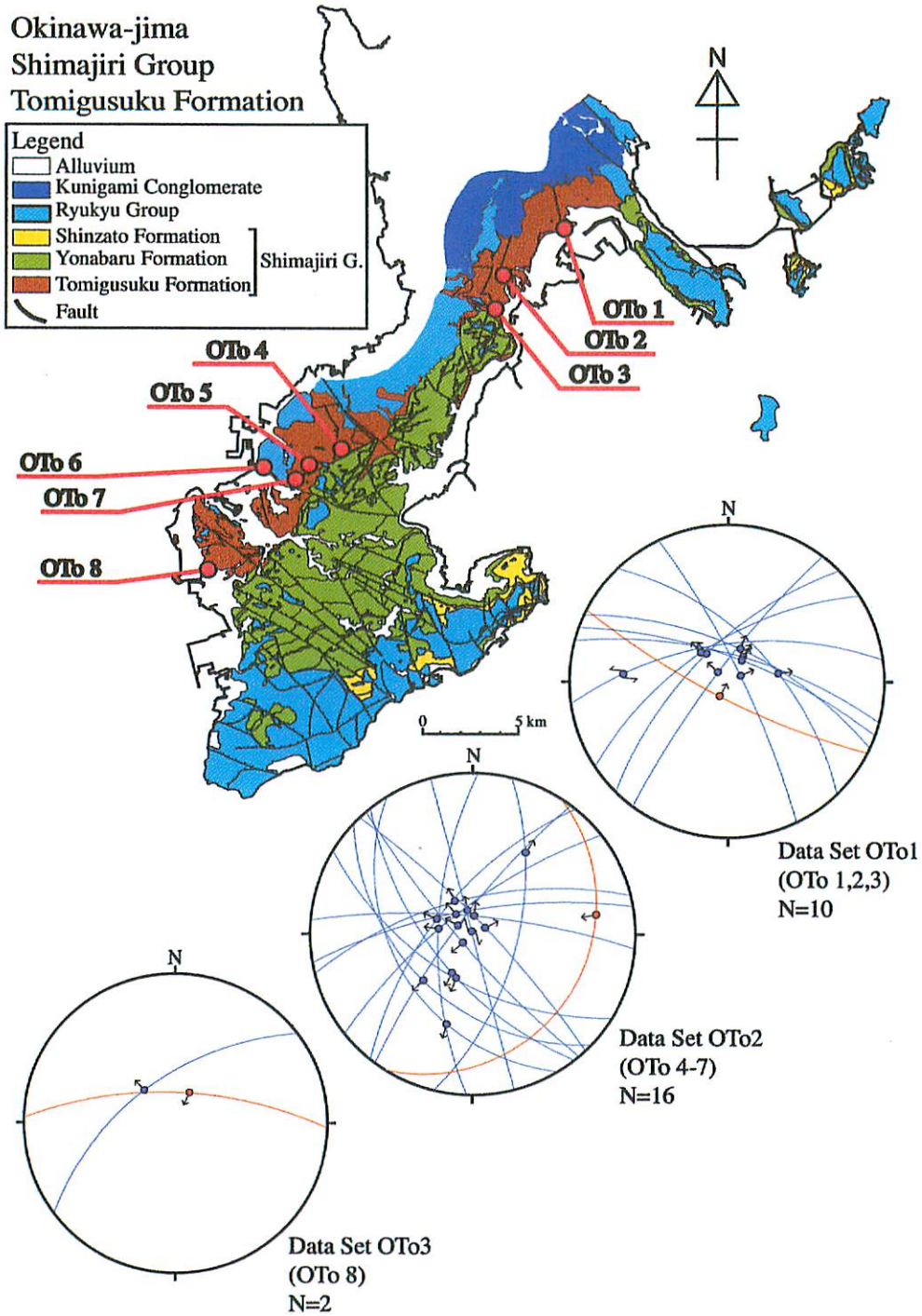

Fig.4. Fault-slip data collected from the Tomigusuku formation in the Okinawa-jima. Other explanations are same as in Fig.4.

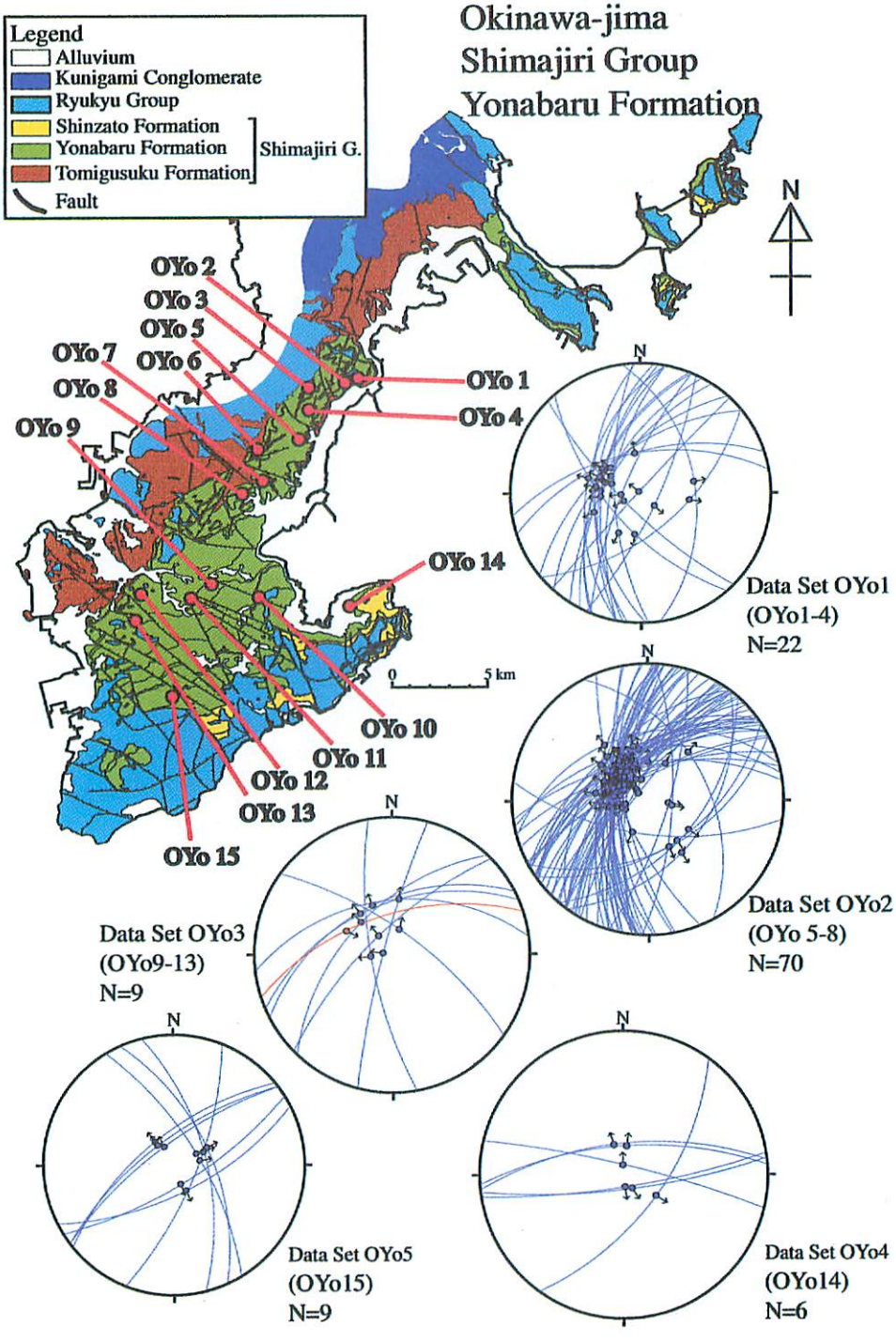

Fig.5. Fault-slip data collected from the Yonabaru formation in the Okinawa-jima. Other explanations are same as in Fig.4.

grouped into one unit for each ca. 5 km square. Most fault data belonging to the formation are the normal fault and dip-slip type.

4.1.3. Shinzato formation

Figure 6 shows the fault-slip data and the site map of the Shinzato formation. 33 fault-slip data are obtained from the formation, which are grouped into three data sets; OSh1 to OSh3. Fault data are grouped into one unit for each ca. 5 km square. Most fault-slip data collected from this formation belong to the normal fault type, while there are some reverse faults.

4.1.4. Ryukyu group

Fault-slip data and site map of the Ryukyu group are shown in Fig. 7. Thirty-six fault-slip data are collected from the group, which are grouped into four data sets; Data Set ORN1, ORN2, ORS1 and ORS2. Fault-slip data are obtained from mainly Naha formation. Fault data are grouped into one unit for each ca. 5 km square. Most type of fault-slip data is normal fault.

4.2. Aguni-jima

Figure 8 shows the fault-slip data and the site map measured in Aguni-jima. 24 fault-slip data are collected from this island. Twelve faults are collected from the Aguni group and also 12 fault slip data from the Ryukyu group. Most of the fault type from the Aguni group is dip-slip normal fault whose strike is clustered to NW-SE. The collected sites of the Ryukyu group are located in the northern part of the island. The faults observed in the Ryukyu group belong to normal fault whose strike is clustered to NE-SW while there is also a cluster NW-SE.

4.3. Kume-jima

Figure 9 shows the fault-slip data and the site map measured in Kume-jima. 26 fault-slip data are obtained from the Shimajiri group and 9 fault-slip data from the Ryukyu group which are grouped into three data sets; KuS1, KuS2 and KuR. Most of the faults observed in the Shimajiri group and the Ryukyu group belong to dip-slip normal fault or oblique normal fault, while some faults are reverse fault. Strike of these faults in the Shimajiri group directs various orientations and the faults in the Ryukyu group direct to NW-SE as a whole.

4.4. Yoron-jima

The fault-slip data and the site map of Yoron-jima are shown in Fig. 10. 38 fault-slip data are obtained from this island. Most of the faults observed in the Ryukyu group belong to dip-slip or oblique normal fault, while some faults are reverse fault. Strike of

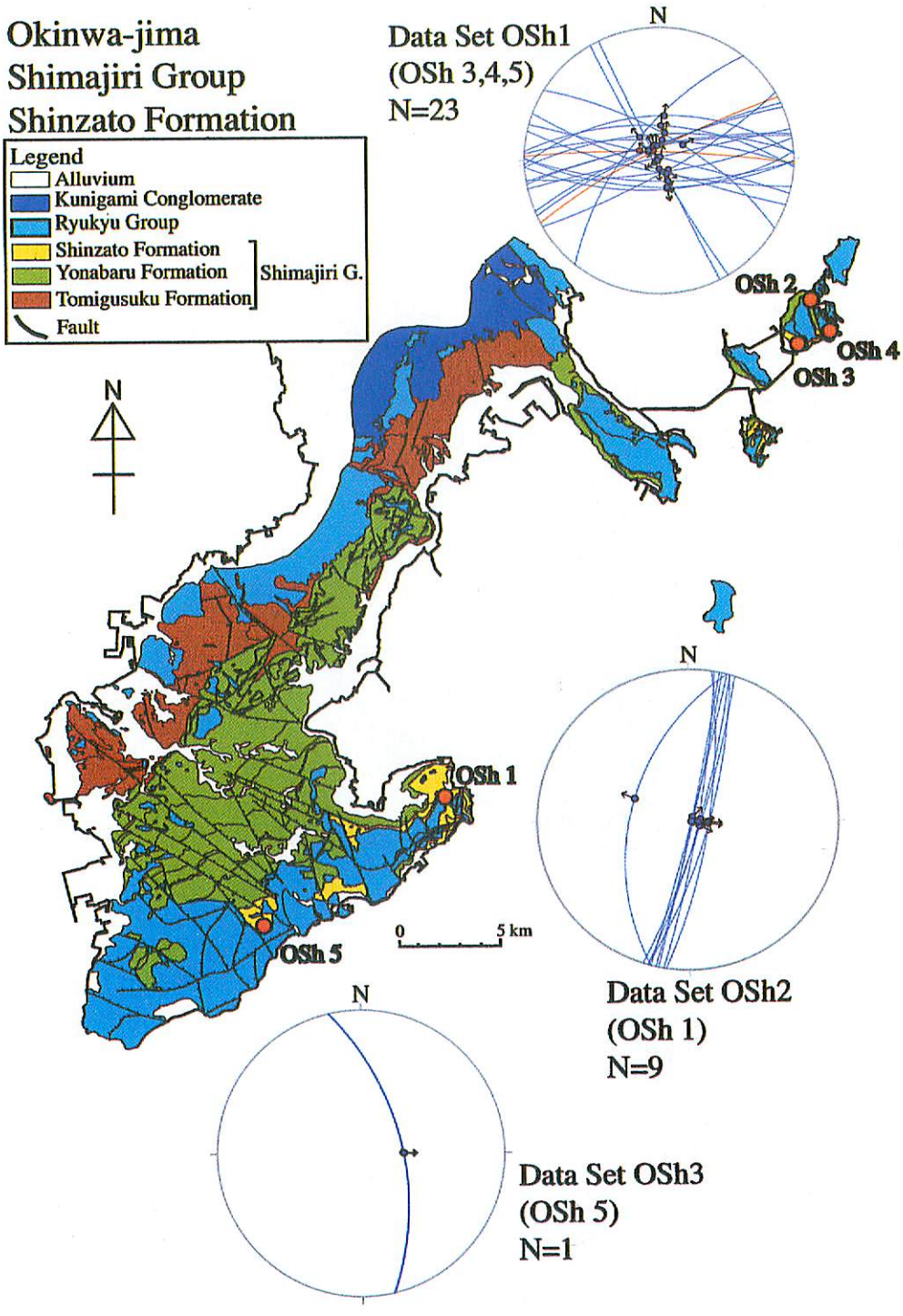

Fig.6. Fault-slip data collected from the Shinzato formation in the Okinawa-jima. Other explanations are same as in Fig.4.

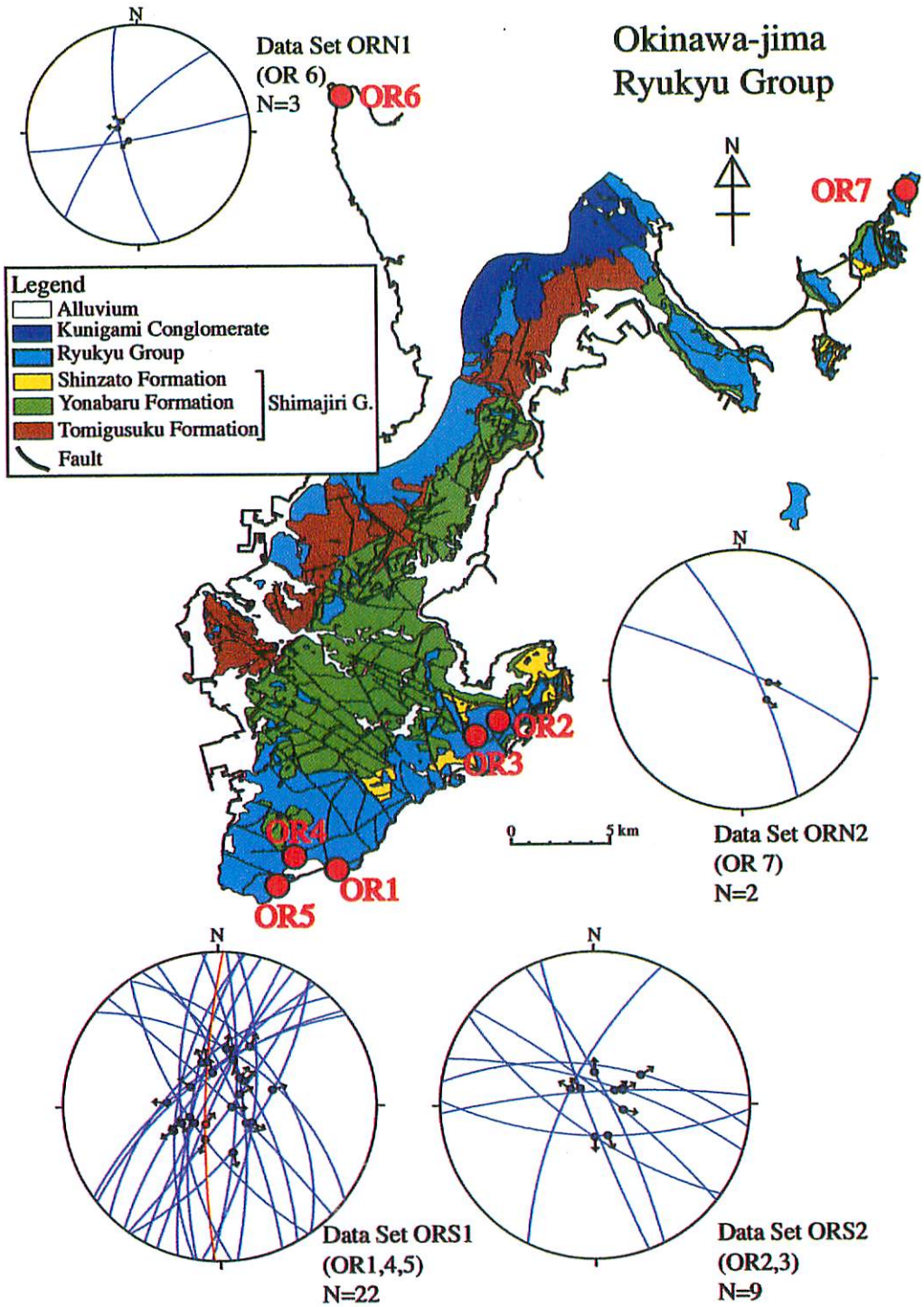

Fig.7. Fault-slip data collected from the Ryukyu group in the Okinawa-jima. Other explanations are same as in Fig.4.

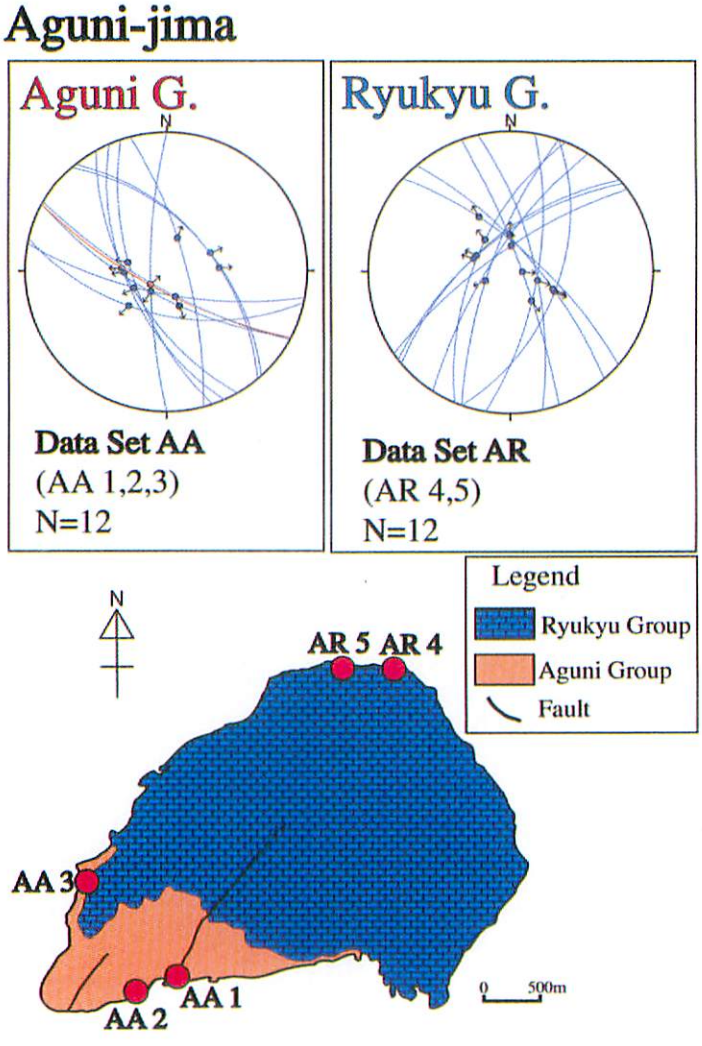

Fig.8. Fault-slip data collected in the Aguni-jima (geology after Kizaki (1985)). Fault-slip data are projected on lower hemisphere, equal area net. Arrows inside the nets indicate the sense of slip. N gives the number of fault-slip data measured at each group.

the faults within the Ryukyu group directs various orientations.

4.5. Okinoerabu-jima

Figure 11 shows the fault-slip data and the site map measured in Okinoerabu-jima. 15 fault-slip data are measured from the Ryukyu group, which are grouped into two data sets; OeR1 and OeR2. Most of the faults in the Ryukyu group belong to dip-slip or oblique normal fault. Strike of most faults observed in the Ryukyu group is ENE-WSW. This direction is similar to that of the active faults in the Okinoerabu-jima.

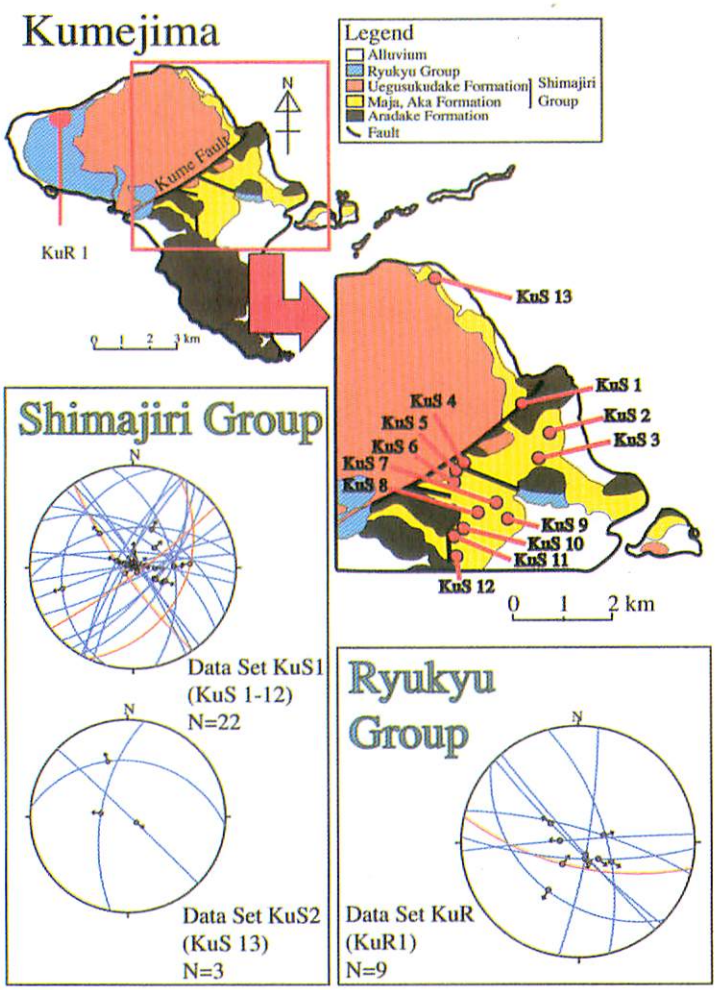

Fig.9. Fault-slip data collected in the Kume-jima. Other explanations are same as in Fig.8.

4.6. Tokunoshima

Figure 12 shows the fault-slip data and the site map measured in Tokunoshima. 35 fault-slip data are collected from the Ryukyu group. Type of fault from the fault-slip data is almost dip-slip or oblique normal fault, while there are some reverse faults. Strike of most faults measured from the Ryukyu group is NW-SE.

4.7. Kikai-jima

Figure 13 shows the fault-slip data and the site map measured in Kikai-jima. 20 fault-slip data are measured from the Shimajiri group and 11 fault-slip data from the Ryukyu group which are grouped into five data sets; KiS1, KiS2, KiS3, KiR1 and KiR2.

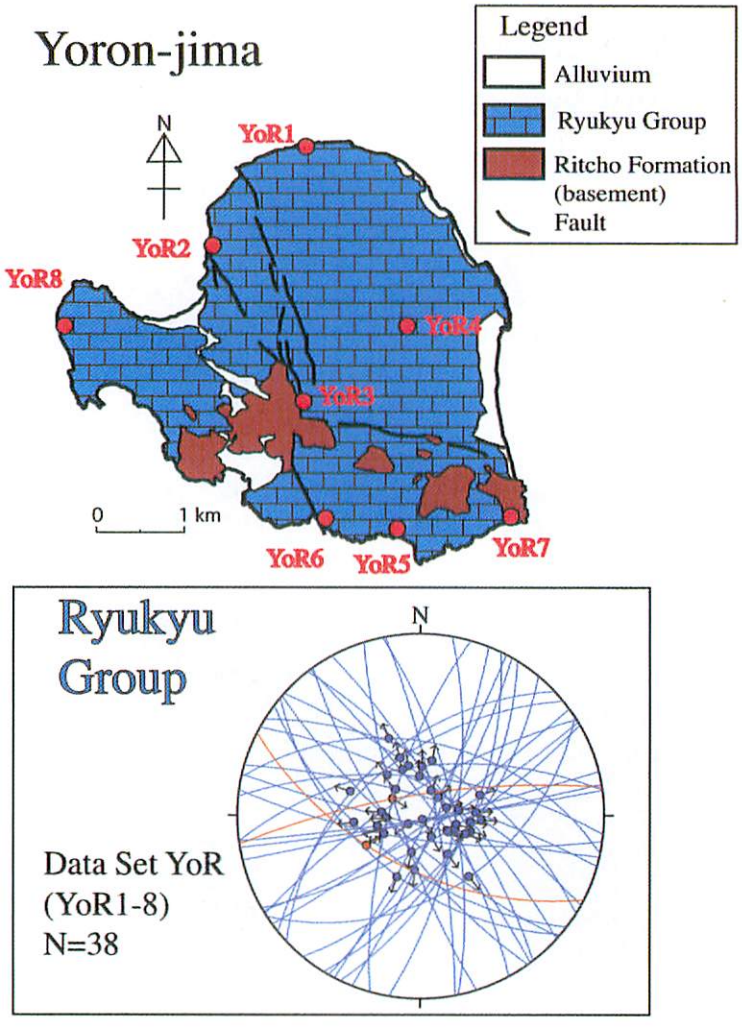

Fig.10. Fault-slip data collected in the Yoron-jima. Other explanations are same as in Fig.4.

Most of the faults observed in the Shimaijri group and Ryukyu group belong to dip-slip or oblique normal fault while some faults are reverse type. Strike of most of the faults observed in the Shimajiri group is ENE-WSW. Strikes of most of the faults collected from the Ryukyu group are clustered to NE-SW.

4.8. Takara-jima

Figure 14 shows the fault-slip data and the site map measured in Okinoerabu-jima. 15 fault-slip data are measured from the Ryukyu group, which are grouped into two data sets; OeR1 and OeR2. Most faults observed in the Takarajima group and Ryukyu group belong to dip-slip or oblique normal fault, while several faults within the Ryukyu

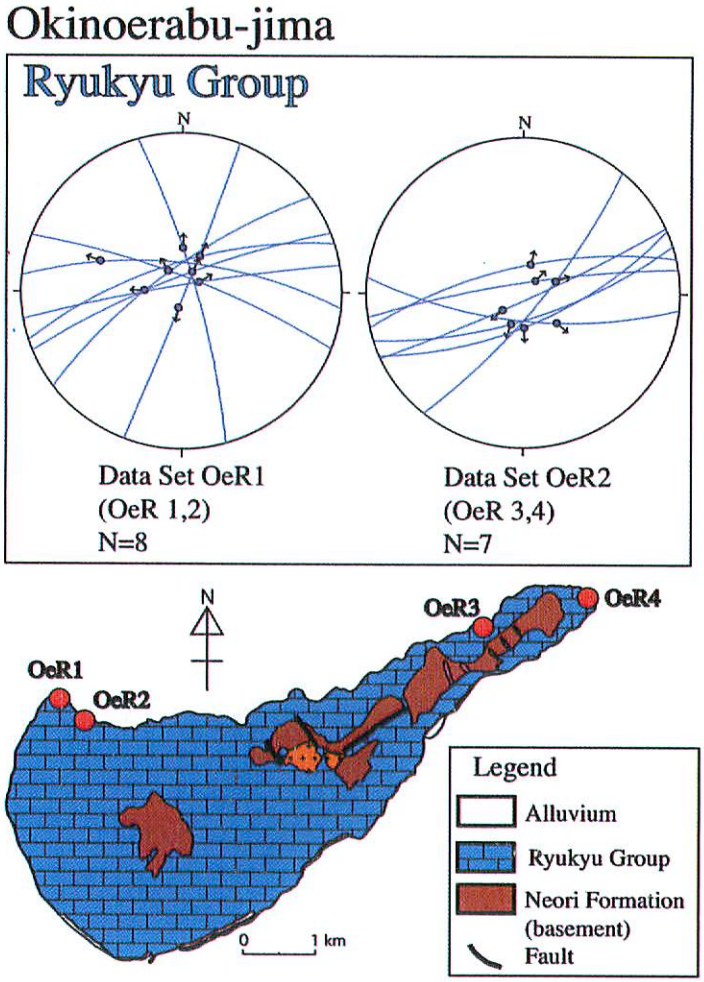

Fig.11. Fault-slip data collected in the Okinoerabu-jima. Other explanations are same as in Fig.4.

groupare reverse type. Strike of the faults observed in the Takarajima group is E-W and that in the Ryukyu group directs various orientations.

4.9. Tanegashima

The fault-slip data and the site map of Tanegashima are shown in Fig. 15. More than 200 fault-slip data are measured, which are grouped into eight data sets; TaT, TaK, TaO1, TaO2, TaO3, TaO4, TaM and TaA.

11 fault-slip data are measured from the Tashiro formation. Most of the faults observed in the Tashiro formation belong to dip-slip or oblique normal fault. Strikes of most of the faults measured in the Tashiro formation are scattered N-S to NW-SE.

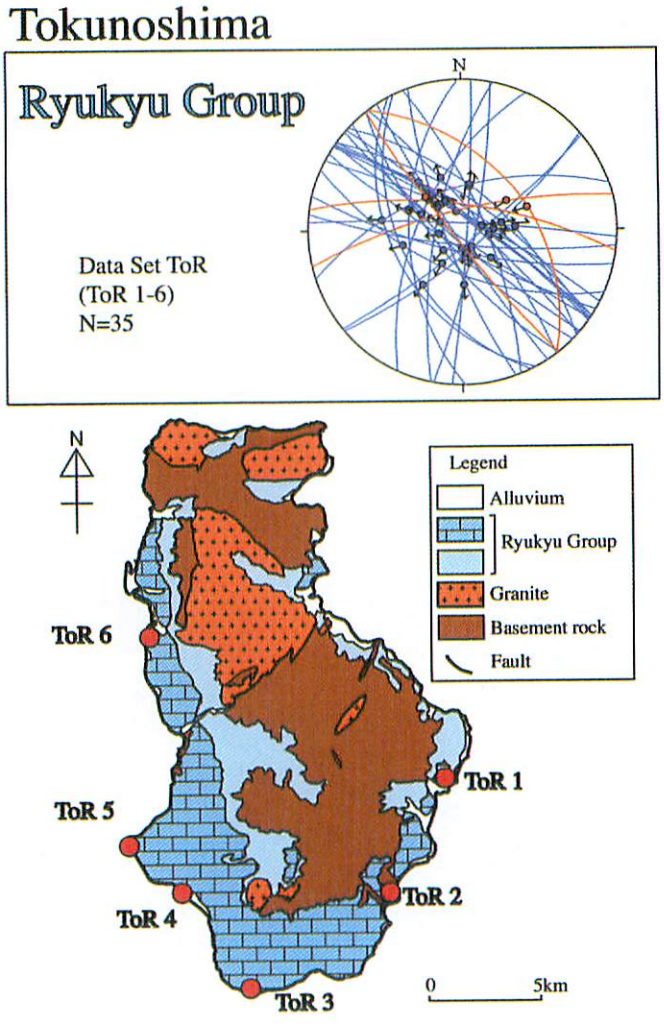

Fig.12. Fault-slip data collected in the Tokunoshima. Other explanations are same as in Fig.4.

17 fault-slip data are collected from the Kawachi formation. Fault type deduced from the fault-slip data is almost normal fault, while there are several reverse faults. Strikes of most of the faults collected from the Kawachi formation are scattered N-S to NW-SE.

More than 150 fault-slip data are obtained from the Osaki formation, which are grouped into four data sets; TaO1, TaO2, TaO3 and TaO4. Grouping are performed for each 5 km square grid. These faults are mostly normal fault, while there are several reverse faults.

15 fault-slip data are measured from the Masuda formation and one fault-slip from the Takenokawa formation. The faults observed in the Masuda and Takenokawa